



## Adsorption of Pesticides onto Granular Activated Carbon: Determination of Surface Diffusivities Using Simple Batch Experiments

S. BAUP, C. JAFFRE, D. WOLBERT AND A. LAPLANCHE

*Laboratoire Chimie des Nuisances et Génie de l'Environnement, Ecole Nationale Supérieure  
de Chimie de Rennes, Avenue du Général Leclerc, F-35700 RENNES, France*

*Received November 3, 1999; Revised April 10, 2000; Accepted May 15, 2000*

**Abstract.** The Homogeneous Surface Diffusion Model (HSDM) has been successfully used to predict the adsorption kinetics for several chemicals inside batch adsorber vessels. In addition to the adsorption equilibrium, this model is based on external mass transfer and surface diffusion. This paper presents the determination of the surface diffusion coefficient ( $D_s$ ) using a differential column batch reactor (DCBR). The adsorption kinetics for three pesticides onto granular activated carbon have been established experimentally. Their corresponding three diffusion coefficients were determined by fitting the computer simulations to the experimental concentration-time data. The results show that this original apparatus increases by an order of magnitude the range of reachable diffusion coefficient compared to perfectly mixed contactors. Moreover the computed  $D_s$  values are more accurate because of the better assessment of the external mass transfer coefficient ( $k_f$ ) for fixed beds.

**Keywords:** liquid adsorption, differential column batch reactor, granular activated carbon, homogeneous surface diffusion model, pesticides, surface diffusivity

### Introduction

Faced with an increasing contamination of natural waters by pesticides, adsorption onto activated carbon has become widely used in drinking water plants. The design of an adsorption treatment has to be based on the transient phenomenon which drives a given dissolved compound towards adsorption sites within the particles of powdered or granular activated carbon. The adsorption capacity, or adsorption equilibrium, is the attractive force. Two resistances hinder the progression of the compound: the crossing of the laminar boundary layer surrounding the particle (the external mass transfer) and the diffusion within the particle (the internal mass transfer). The latter can be a diffusion in the liquid phase contained in the pores or a diffusion of the molecules in the adsorbed state at the pore's surface. According to Komiyama and Smith (1974), the main diffusion mechanism is the surface diffusion. The used model combines external mass transfer and surface

diffusion (the latter phenomenon is usually called HSDM for Homogeneous Surface Diffusion Model).

The characteristic parameter for the external mass transfer, the coefficient  $k_f$ , is likely to be estimated by semi-empirical equations. On the contrary, the surface diffusion coefficient  $D_s$  depends highly on the nature of the activated carbon, its structure, its preparation (raw material, calcination, activation), and on the nature and size of the adsorbed compound. Actually, only limited data is available and the large variability observed does not plead for a reliable correlation in the near future. The value of the surface diffusion coefficient has therefore to be obtained by fitting a HSDM model to some experimental data.

In order to obtain surface diffusivity values for some pesticides, kinetic experiments will be carried out with a differential column batch reactor (DCBR) rather than classical batch adsorber vessels. Described by Hand et al. (1983), this original apparatus, easy to set up, was chosen so that  $k_f$  effect could be minimised or, at

least, well defined. This results in more accurate  $D_s$  estimations. Once  $D_s$  is obtained for a given compound and a given activated carbon, it can be used in various adsorption treatments, like powdered activated carbon addition or granular activated carbon beds, where the same compound has to be adsorbed onto the same carbon.

## Theory

### Adsorption Theory

It is widely accepted that the process of adsorption can be represented by four consecutive steps (Noll et al., 1992). Figure 1 describes the progression of a molecule of adsorbate from the bulk towards the site of adsorption.

It is important to note that intraparticle mass transfer involves two different phenomena: porous diffusion (the adsorbate first diffuses in the liquid filling the pores and then is adsorbed) and surface diffusion (the adsorbate is first adsorbed then diffuses from one site to another).

The convective progression of step 1 appears to be very fast compared to the diffusion through the outer layer and within the particle. The concentrations of the liquid bulk will only be governed by the overall mass balance and the hydraulic behaviour of the vessel. An instantaneous reversible reaction is assumed for the

real adsorption step (step 4). The liquid phase concentration of adsorbate and the adsorbate load at the carbon's surface are locally related by an equilibrium law. Thus adsorption kinetic is governed by external mass transfer and internal diffusion i.e. by the coefficients  $k_f$ ,  $D_p$  and  $D_s$ . In order to simplify simulations, models that take into account only two coefficients were developed. As noticed by Komiyama and Smith (1974), the contribution of  $D_s$  is 20 times as important as the  $D_p$  contribution. Later, in a review paper, Al Duri (1996) mentioned several other authors confirming this observation. Therefore a model based only on  $k_f$  and  $D_s$  will be used here.

### The External Mass Transfer

The mass transfer through a diffusional boundary layer is represented by a linear driving force model, characterized by the coefficient  $k_f$ . This phenomenon occurs in numerous processes, not only adsorption but also catalysis for instance. It has been widely documented and, in various situations, empirical equations are now available. They give  $k_f$  as a function of the hydraulic behaviour in the vessel or in the surrounding of the particle, some physical properties of the solvent and the molecular diffusion of the solute (Noll et al., 1992; Ruthven, 1984). The  $k_f$  value is only affected by the particle size, but not by the nature or the porosity of the GAC.

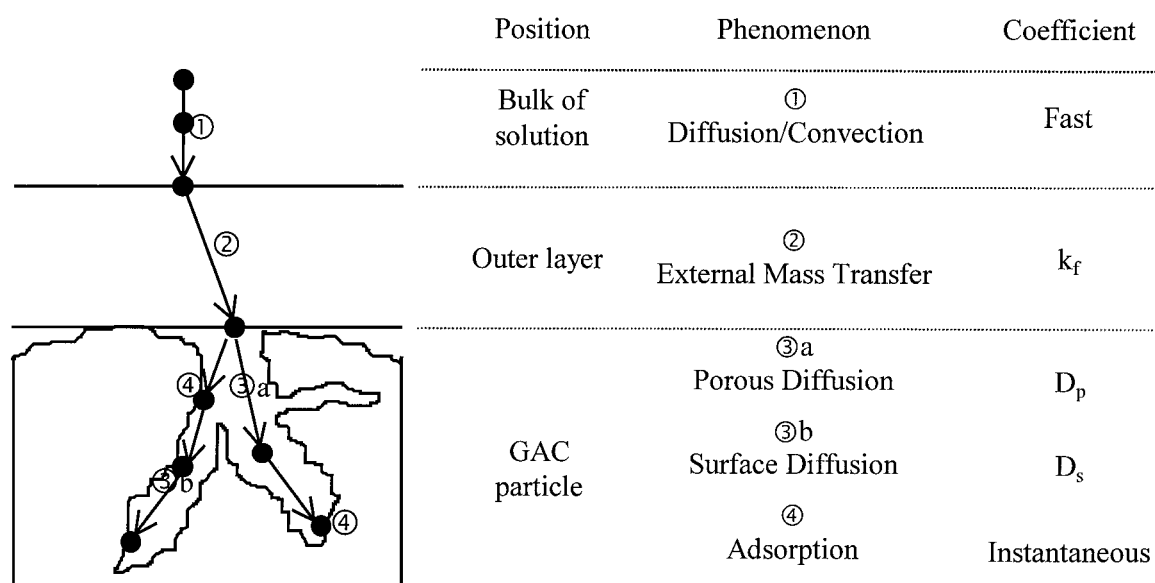


Figure 1. The four steps of adsorption (adapted from Weber and Smith, 1987).

It should be noticed however that for non-ideally stirred vessels the  $k_f$  value will depend on issues like vessel shape, position, velocity, and type of stirrer, distance between stirrer and particle, and also particle size and density. As a result, one has usually to deal with a  $k_f$  distribution rather than a unique value.

Furthermore the molecular diffusion coefficient,  $D_{mol}$ , is needed for Sh and Sc numbers calculation. Several correlations, cited by Crittenden et al. (1987) and Noll et al. (1992), are likely to estimate  $D_{mol}$ .

#### *Simplified Model of Adsorption: Homogeneous Surface Diffusion Model*

Initiated by Rosen (1952), HSDM was first resumed by Weber and Chakravorti (1974). This model is also described as the Film-Solid Diffusion Model (Al Duri, 1996). The main hypothesis of HSDM is that porous diffusion is neglected, so that internal mass transfer is only due to surface diffusion. The HSDM assumptions are therefore the following:

1. the contactor's mass balance: according to our experiments, the mass balance of a discontinuous perfectly mixed vessel will be used.
2. internal mass transfer is only governed by surface diffusion.
3. external mass transfer is governed by a linear driving force.
4. at the solid/liquid interface, there is continuity between external mass transfer and internal diffusion.
5. at the solid/liquid interface, there is equilibrium between adsorbate concentration in the fluid and adsorbate load on the surface.
6. the particle of adsorbent is supposed to be spherical and homogeneous.

Some authors (Ruthven, 1984; Zhou and Martin, 1995) describe a relationship between final equilibrium surface loading and average surface diffusivity. However, the real influence is onto the local value of the surface diffusivity and is a result of the local surface load at any given time. Its mathematical expression and the leading parameters are very difficult to establish and to estimate, especially for complex surfaces like activated carbon. For this reason, surface diffusivity will be assumed to be independent of the surface loading in HSDM. A dimensionless ratio can be defined, the Biot Number, which compares the initial external mass transfer for a nonloaded particle with an estima-

tion of the initial surface diffusion for a particle without boundary layer (Noll et al., 1992; Roy et al., 1993). In other words, the largest possible external mass transfer rate is compared to the largest possible diffusion rate for a given situation. This dimensionless number has the following form:

$$\text{Biot} = \frac{k_f R_p C_0}{D_s \rho_a Q_0^*}$$

Traegner and Suidan (1989) noticed 3 typical cases:

- Biot  $\gg 100$ , surface diffusion will always be the rate limiting mechanism, thus simulation results are very sensitive to  $D_s$  variations and insensitive to  $k_f$  variations. Clearly these conditions are not suitable for the determination of the external mass transfer coefficient by fitting the simulation to experimental data.
- Biot  $\ll 1$ , external mass transfer always enforces its rate, thus simulation results are very sensitive to  $k_f$  variations and are insensitive to  $D_s$  variations. Clearly such experiments contain no information about the surface diffusion coefficient.
- Biot  $\in [1; 100]$ , both mechanisms are important, so model is sensitive to  $k_f$  and  $D_s$ . In this paper, the lower limit of the Biot number for the  $D_s$  determination will be established for a typical use in water treatment.

#### *Equations of Homogeneous Surface Diffusion Model*

The mathematical translation of the previous hypotheses is shown step by step in the following set of equations.

1. The overall mass balance for a discontinuous perfectly mixed vessel is:

$$\frac{dC_b}{dt} = -W \frac{dq_{avg}}{dt} \quad (1-1)$$

where  $C_b$  is the liquid concentration of adsorbate in the bulk and  $W$  the GAC dosage (mass of carbon per liquid volume unit).

$q_{avg}$  is the GAC average load and is calculated by the following equation:

$$q_{avg} = \frac{3}{R_p^3} \int_0^{R_p} q(r, t) r^2 dr \quad (1-2)$$

with  $q(r, t)$  the load profile along the radius at time  $t$ .

2. The internal mass transfer is in accordance with Fick's first law, so that:

$$\frac{\partial q(r, t)}{\partial t} = \frac{D_s}{r^2} \frac{\partial}{\partial r} \left( r^2 \frac{\partial q(r, t)}{\partial r} \right) \quad (2)$$

Boundary condition n°1:

$$\frac{\partial q(r, t)}{\partial r} = 0 \quad \text{at } r = 0, \forall t$$

This boundary condition expresses the spherical symmetry of the adsorbent particle (assumption n°6). As a consequence, no adsorbate molecule crosses the centre of the particle.

- 3 and 4. Continuity at the solid/liquid interface between external mass transfer and internal transport corresponds to the boundary condition n°2:

$$\rho_a D_s \frac{\partial q(r, t)}{\partial r} = k_f (C_b - C_s) \quad \text{at } r = R_p \quad (3)$$

In Eq. (3), the left-hand term expresses the transfer due to surface diffusion whereas the right-hand term corresponds to the external mass transfer. The two transfer rates have to be equal at the adsorbent surface at any time.

5. Equilibrium at the solid/liquid interface is expressed by semi-empirical laws. Single solute adsorption can be described by usual models i.e. Freundlich and Langmuir equations (two fitted parameters) or Redlich-Peterson and Jossens-Myers equations (three fitted parameters) (Zhou, 1992).

Finally, the initial conditions specify that fresh GAC is added to a solution with an initial solute concentration  $C_0$ :

$$C_b(t) = C_0; C_s(t) = 0; q(r, t) = 0 \quad \text{at } t = 0, \forall r$$

A computer program developed in our laboratory solves the HSDM equations. An orthogonal collocation method is used to transform the partial differential equation into a set of ordinary differential equations (Villadsen and Stewart, 1967; Roy et al., 1993). A fourth order implicit integration method solves the algebraic-differential equation system and produces, as result, the time evolution of the bulk concentration and of the load profile along the grain radius. The current

version of the code does not yet perform an automatic search for the  $D_s$  value based on some experimental data using a least square adjustment method. For the time being, this is done manually.

## Experiments

### Activated Carbon

We used a commercial granular activated carbon, widely used in water treatment plants: F400 provided by CHEMVIRON.

For its preparation, the GAC was first washed with ultra-pure water to remove fines, then plunged into ultra-pure water for 4 hours in order to eliminate possibly adsorbed organics. After being oven-dried at 105°C, the GAC is stored in a desiccator under vacuum conditions. For adsorption isotherms, the GAC was crushed. For DCBR studies, GAC is sieved into several particle size fractions and experiments were conducted with the main size fraction: diameter in the 1.00 to 1.25 mm range.

### Pesticides

Experiments were conducted with three pesticides: atrazine, bromoxynil and diuron. They are pure and technical products.

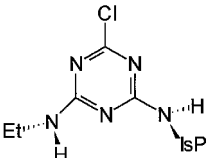
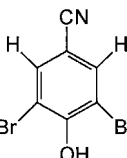
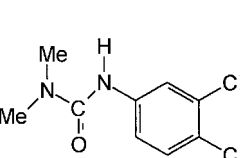
A 10 mg · L<sup>-1</sup> stock-solution was prepared by dissolving each pesticide in ultra-pure water. This solution is stirred during 3 days in darkness to complete dissolution. Then dilute solutions were prepared from this mother-solution.

The choice of these pesticides was motivated by two reasons. First, they are not only widely used but they also appear more and more often at critical concentrations in raw water supplies. Secondly, they belong to different pesticide families, with potentially different behaviours towards the activated carbon. Table 1 shows their structure.

### Adsorption Isotherms

Adsorption isotherm experiments were conducted with the usual bottle-point method. Varying and accurately determined amounts of crushed GAC were added to four out of five 2.5 L bottles containing 2 L of pesticide solution, the remaining bottle being used as reference. Bottles were sealed and magnetically stirred for 5 days

Table 1. Structure of the chosen pesticides.

	Atrazine	Bromoxynil	Diuron
Class	s-triazine	nitrile	substituted urea
Structure			

at 25°C. After 5 days, residual liquid concentrations were analyzed and adsorbate loads were derived from the mass balance. Adsorption isotherms are described by the Freundlich equation:

$$q_s = KC_s^{1/n}$$

For each pesticide, two series of experiments were performed at two different initial concentrations. Table 4 summarizes the initial concentrations of pesticide and the varying amounts of crushed GAC.

#### Differential Column Batch Reactor

Adsorption kinetic experiments were carried out with a differential column batch reactor. Hand et al. (1983) and Noll et al. (1992) described this apparatus. A pesticide solution is pumped from a stirred tank and flows through a small column that contains GAC. Then the solution is directed back to the tank. Figure 2 presents this apparatus.

Tank, column and flowmeter are made of glass. The total volume of pesticide solution contained in the tank is 5 L. The column, whose internal diameter is 8 mm,

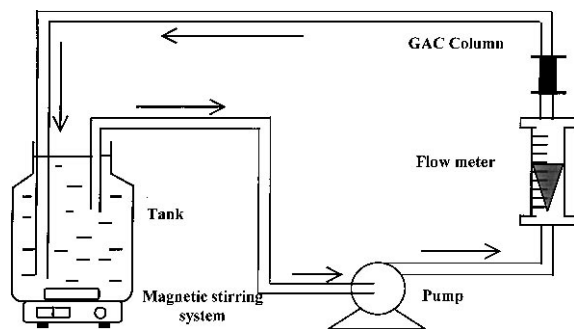


Figure 2. Principle of a Differential Batch Column Reactor.

is filled with 100 mg of GAC. The gear-pump is made of stainless steel and PTFE while tubing are made of polyamide. The choice of these materials was made in order to avoid any interference adsorption likely to alter our results. The pump provides a 100 L · h<sup>-1</sup> flow, that is checked by the flowmeter. The whole unit is kept in darkness and at room temperature.

One advantage of DCBR apparatus is that, for high flowrates, it closely approaches the Discontinuous Perfectly Mixed Tank Reactor concept. As a consequence, we are allowed to use the overall mass balance [1-1] given above. It is mainly a means to gain some control over the turbulent flow pattern, which affects the external transfer, surrounding all the particles.

For classical adsorption kinetics, external mass transfer coefficient can be deduced from the first few minutes of adsorption (Walker and Weatherley, 1999; Ganguly and Goswamy, 1996). Nevertheless, some difficulties in  $k_f$  estimations may occur due to the choice of the first time interval used for  $k_f$  calculations or experimental uncertainties. In a DCBR, the GAC is set up like in a fixed bed, the external mass transfer coefficient can, therefore, be estimated using the more reliable  $k_f$  correlations for fixed beds. In addition, the influence of external mass transfer can be reduced by increasing the flowrate. Note that for  $k_f$  calculation, Hand et al. (1983) advocated the semi-empirical equation of Wakao and Funazkri (1978) for DCBRs. This correlation, developed for fixed-beds, takes the following form:

$$Sh = 2 + 1.1 Re^{0.6} Sc^{1/3}$$

The experimental conditions are summarized in Table 2.

About 20 samples, each of them of 5 mL, are taken for analysis during a kinetic experiment. Thus, the total volume withdrawal represents about 2%, that is neglected and does not cause significant adsorbent enrichment.

Table 2. DCBR conditions.

	Atrazine	Bromoxynil	Diuron
Flow ( $\text{L} \cdot \text{h}^{-1}$ )	100	100	100
Tank volume (L)	5	5	5
GAC density ( $\text{kg} \cdot \text{m}^{-3}$ )	750	750	750
Mean particle radius (mm)	0.5625	0.5625	0.5625
CAG mass (mg)	100.2	100.0	100.7
$C_0$ ( $\mu\text{g} \cdot \text{L}^{-1}$ )	481.1	715.6	471.1
Duration (days)	3	5	3

Table 3. Analytical conditions.

	Atrazine	Bromoxynil	Diuron
Wavelength (nm)	220	288	245
Eluant composition (% v/v)	55/45	70/30	55/45
Eluant flow ( $\text{ml} \cdot \text{min}^{-1}$ )	0.8	0.7	0.8
Retention time (min)	13	2.7	12.5

### Analysis

Pesticide concentrations are measured by High Performance Liquid Chromatography coupled with an UV diode array photodetector. Samples are filtered (MILLIPORE Millex HV25,  $0.45 \mu\text{m}$ ) before injection.

The WATERS HPLC line is composed by the following elements:

- pump controller 600.
- autosampler 717 (injection loop:  $50 \mu\text{L}$ ).
- guard column.
- C18 SYMMETRY<sup>®</sup> column (p.d.  $5 \mu\text{m}$ ; length 250 mm; i.d. 4.6 mm) for atrazine and diuron or CN NUCLEOSYL<sup>®</sup> column (p.d.  $10 \mu\text{m}$ ; length 250 mm; i.d. 4.6 mm) for bromoxynil

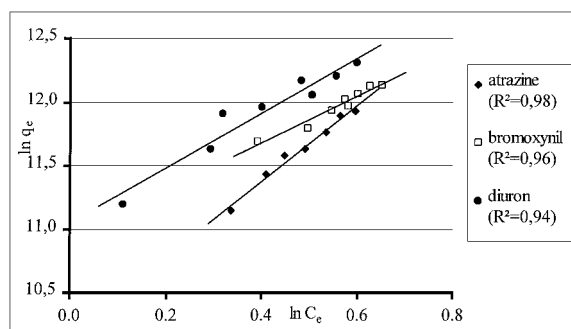


Figure 3. Freundlich representation for the pesticides.

- photodiode array UV detector 996.
- software MILLENIUM<sup>®</sup>.

Analyses are performed with a water/acetonitrile eluant. Table 3 shows the analytical conditions.

## Results and Discussion

### Adsorption Equilibrium

The adsorption equilibrium of a pure compound does depend on the abundance of possible adsorption sites as well as site accessibility. Therefore geometrical considerations: pore size distribution and tortuosity, functionalities of activated carbon and adsorbate can affect the isotherm results. For the three studied pesticides, adsorption isotherm results and corresponding Freundlich modelisations are respectively shown in Fig. 3 and Table 4.

Diuron is more adsorbed than atrazine. This can be explained by the structure of the molecule. The diuron molecule appears to be more linear and flat than a molecule of atrazine because of an electron delocalization that stiffens the urea part and, consequently,

Table 4. Equilibrium: conditions (initial concentration; crushed GAC amount) and results.

	Atrazine	Bromoxynil	Diuron	
$C_{01}$ ( $\mu\text{g} \cdot \text{L}^{-1}$ )	259.0	454.8	261.1	
$C_{02}$ ( $\mu\text{g} \cdot \text{L}^{-1}$ )	498.8	817.5	558.1	
	Bottle 1	Bottle 2	Bottle 3	Bottle 4
Crushed GAC amount ( $\text{mg} \cdot \text{L}^{-1}$ )	0.7	1.5	2.3	3.1
	Atrazine/F400	Bromoxynil/F400	Diuron/F400	
$K$ [ $(\mu\text{mol} \cdot \text{g}^{-1}) \cdot (\mu\text{mol} \cdot \text{L}^{-1})^{-1/n}$ ]	607.2	573.0	875.2	
$n$ (dimensionless)	3.38	5.42	4.63	

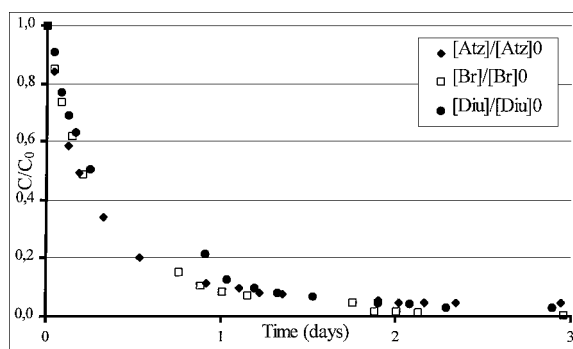


Figure 4. Adsorption of pesticides onto DCBR.

keeps it in the plane of the phenyl group. On the other hand, the ethyl and isopropyl group of atrazine cannot be placed in the plane of the triazine because of steric hindrance. So that atrazine is less linear and more voluminous than diuron. For bromoxynil, the molecule is slightly larger than the diuron molecule, but has a greater functional variability than atrazine and hence a broader range of possible sites.

For the HSDM model, the equilibrium has to be determined at the particle surface. The Freundlich adsorption isotherm model was the best fit among the two parameters models. The three parameters models did not improve the least square criteria and were therefore disregarded.

These parameters are specific to a given compound—activated carbon couple.

#### Differential Column Batch Reactor Kinetics

The three experimental DCBR kinetics are presented Fig. 4 in reduced form: relative pesticide concentration versus time. The abbreviation Atz, Br and Diu are respectively used for atrazine, bromoxynil and diuron. [Atz] represents the atrazine liquid concentration and [Atz]₀ the initial concentration.

Roughly speaking, atrazine and bromoxynil seem to have the same behaviour while the adsorption rate for diuron appears slower. Equilibrium is reached after two

to three days. Before any  $D_s$  determination, we need to evaluate the external mass transfer coefficient to be used in the model for each pesticide. Using the Wakao and Funazkri (1978) correlation,  $k_f$  values have been estimated for the three pesticides (see Table 5).

These values are, on average, one order of magnitude greater than  $k_f$  values observed for classical batch stirred reactors. For instance, for experiments carried out inside a batch adsorber vessel, Walker and Weatherley (1999) obtained  $2.8 \times 10^{-3} \text{ cm} \cdot \text{s}^{-1}$  for an acid dye, Ganguly and Goswamy (1996) got  $2.5 \times 10^{-3} \text{ cm} \cdot \text{s}^{-1}$  for acetic acid whereas Traegner and Suidan (1984) measured  $6.6 \times 10^{-3} \text{ cm} \cdot \text{s}^{-1}$  for PNP. The external mass transfer will significantly less limit the overall mass transfer rate in DCBRs than in usual batch vessels, even though we are fundamentally facing two identical reactors.

#### Discrimination Efficiency of the DCBR Model

As mentioned before, a minimal Biot number exists below which it will not be possible to determine any surface diffusion coefficient since the observed overall transfer rate will mainly be governed by the external transfer. The same happens to the simulations. In order to estimate that Biot number, we performed several kinetic calculations with various  $D_s$  values, in particular one with an exceptionally high  $D_s$  as an example of a kinetic limited only by the external transfer. The value of the corresponding  $D_s$  was chosen at  $10^{-6} \text{ cm}^2 \cdot \text{s}^{-1}$ . This last calculation will be used as reference against which the other kinetics will be compared. The comparison criteria is an average relative deviation, derived from a least square criteria, defined as follow:

$$S(\%) = 100 \cdot \sqrt{\frac{1}{N} \sum_{i=1}^N \left( 2 \frac{C_{\text{ref}}(t_i) - C(t_i)}{C_{\text{ref}}(t_i) + C(t_i)} \right)^2} \quad (4)$$

Note that the farther  $D_s$  is from the  $D_s$  reference, the farther are the corresponding curves and, as a consequence, the greater is the comparison criteria  $S$ .

Table 5. Kinetics:  $D_s$  and  $k_f$  values.

	Atrazine	Bromoxynil	Diuron
$D_s \text{ (cm}^2 \cdot \text{s}^{-1}\text{)}$	$5.0 \pm 0.8 \times 10^{-10}$	$4.0 \pm 0.7 \times 10^{-10}$	$6.5 \pm 2.6 \times 10^{-11}$
$k_f \text{ (cm} \cdot \text{s}^{-1}\text{)}$	$2.75 \times 10^{-2}$	$2.60 \times 10^{-2}$	$2.70 \times 10^{-2}$
Biot	12.0	18.9	61.9
Mean relative deviation	12.9	8.6	10.7

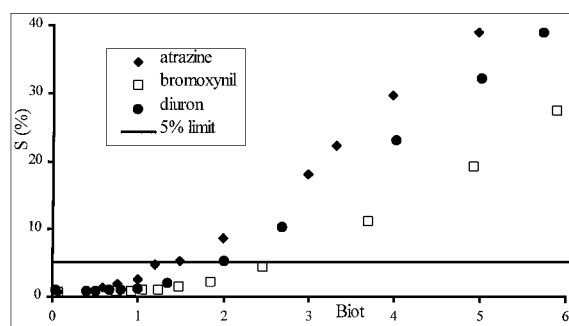


Figure 5. Relative mean deviation between a kinetic with surface diffusion and one without surface diffusion versus Biot number.

In Fig. 5, the evolution of the criteria  $S$  as a function of the Biot number is drawn for the three pesticides. The faculty to discriminate between two  $D_s$  values, when the experimental results are compared to the two simulations, will depend on the experimental measurement error for the concentrations. An average experimental error of 5% is arbitrarily assumed. Any two calculated kinetics, whose gap is within 5%, can not be statistically differentiated when compared to experimental results. As can be seen Fig. 5, below a certain Biot number, all the kinetics are within that 5% gap, thus defining a minimal differentiable Biot value. That critical value is not exactly the same for all the pesticides because adsorption equilibrium does also have an influence on mass transfer ( $\text{Biot}_{\text{Atz}}^{\text{lim}} \approx 1.40$ ,  $\text{Biot}_{\text{Br}}^{\text{lim}} \approx 2.60$ ,  $\text{Biot}_{\text{Diu}}^{\text{lim}} \approx 1.95$ ). These values are in accordance with the segmentation proposed by Traegner and Suidan (1989) and presented in the theoretical part of this paper. If we reconsider the fact that  $k_f$  values for DCBRs are one order of magnitude greater than for usual stirred vessels, it follows that DCBRs allow for the determination of  $D_s$  values about one order of magnitude greater than stirred vessels.

Expressed in terms of  $D_s$ , this means also that a maximal obtainable  $D_s$  value can be defined for a given situation, i.e.  $k_f$ ,  $R_p$ ,  $C_0$ ,  $q_0$ ,  $\rho_a$  being constant. For our experimental conditions, maximal obtainable  $D_s$  values are in the range  $3 \times 10^{-9}$  to  $6 \times 10^{-9} \text{ cm}^2 \cdot \text{s}^{-1}$ . Figure 6 shows, as an example, the comparison criteria as a function of  $D_s$ .

It can be noticed that the comparison criteria is more and more sensitive to  $D_s$  as it decreases. Furthermore, an estimation of an uncertainty range for  $D_s$  can be deduced using the curve of Fig. 6. Let's assume that the best fit for a kinetic was obtained for a  $D_s = 1 \times 10^{-9} \text{ cm}^2 \cdot \text{s}^{-1}$ . According to Fig. 6, this

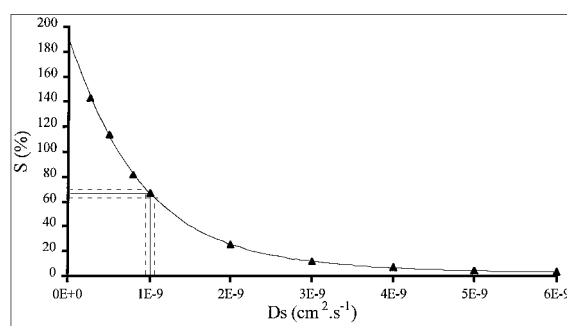


Figure 6. Relative mean distance between a kinetic with surface diffusion and one without surface diffusion as a function of the  $D_s$ .

corresponds to a 66.6% relative mean deviation compared to an “external transfer only” kinetic. If we also assume that we have to deal with an experimental error of 5%, meaning that the real kinetic might well be, on average, 5% above (slower) or below (faster) the measured one. The relative mean deviation of the real kinetic should be between 61.6% and 71.6%. Using again Fig. 6, we end up with a  $D_s$  uncertainty range from  $0.93 \times 10^{-9}$  to  $1.07 \times 10^{-9} \text{ cm}^2 \cdot \text{s}^{-1}$ .

#### Estimation of the Surface Diffusion Coefficient

For the bromoxynil adsorption in a DCBR, an example of HSDM sensitivity towards  $D_s$  is given Fig. 7. Simulations are performed for increasing values of surface diffusivity.

To determine the  $D_s$  value for pesticides, computer simulations are achieved with different  $D_s$ . A manual minimisation is performed with a fitting criteria similar to [4] where the reference is given by the experimental data. When experimental data and simulation curve are in good agreement, the  $D_s$  value is accepted.

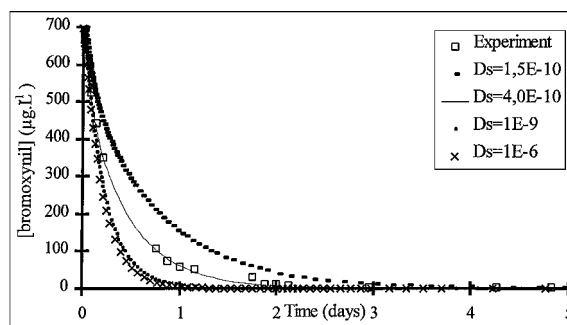


Figure 7. Simulation of bromoxynil adsorption for different  $D_s$  ( $\text{cm}^2 \cdot \text{s}^{-1}$ ).



Table 6.  $D_s$  values for different organic compounds.

Reference	Compound	$D_s$ ( $\text{cm}^2 \cdot \text{s}^{-1}$ )
Ganguly and Goswamy (1996)	Acetic acid	$6.0\text{--}8.5 \times 10^{-7}$
Traegner and Suidan (1984)	<i>para</i> -nitrophenol	$1.92 \times 10^{-8}$
Walker and Weatherley (1999)	Acid dye	$1.5 \times 10^{-9}$
Mc Kay and Al Duri (1991)	Red dye; Yellow dye	$1.3 \times 10^{-10}$ ; $8.5 \times 10^{-11}$

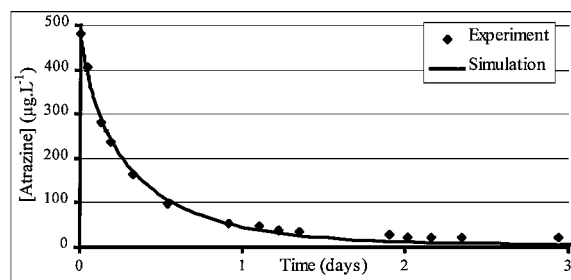


Figure 8. Simulation of atrazine adsorption.

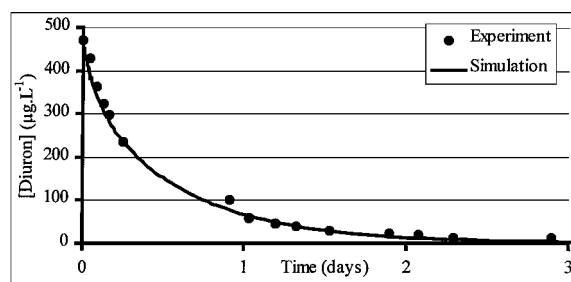


Figure 9. Simulation of diuron adsorption.

The data, corresponding to the asymptotic limit of the kinetic has not been systematically accounted for in the criteria. They solely express the equilibrium finally reached. Unfortunately, slight differences can sometimes be observed between the equilibrium predicted by the model, based on crushed GAC isotherms, and the true GAC equilibrium. These differences, being not related to any kinetic behaviour, are disregarded by restraining the criteria to the evolving part of the kinetic.

Figures 8 and 9 show DCBR kinetics and simulations for the two other pesticides, respectively atrazine and diuron.

For each pesticide, the  $D_s$  value, as well as its uncertainty range, is given Table 5 with the calculated  $k_f$ , the corresponding Biot number and the fitting criteria.

The identified Biot numbers are well above the discrimination limits discussed earlier. This implies that surface diffusion does have a overwhelming impact

on the adsorption kinetic of the described experiments. The experimental data are therefore suitable for  $D_s$  determination.

Using a batch stirred reactor, Qi et al. (1994) studied adsorption of atrazine onto F400 powdered activated carbon. In deionized-distilled water, they obtained  $1.32 \times 10^{-12} \text{ cm}^2 \cdot \text{s}^{-1}$  for atrazine  $D_s$ , that is 100 times smaller than our computed value. This difference can be explained since the authors used a  $D_s$ -only model.

Table 6 gives values of  $D_s$  for several organic compounds. Studies mentioned in this table were carried out with GAC in classical batch stirred adsorbers.

These values cover a large range, because they deal with different families of organic compounds. For these molecules, the volume and the functionalities are disparate, which can explain this large range. It can also be noted that for huge molecule (like red and yellow dye)  $D_s$  is significantly smaller than for little molecules (acetic acid). The three studied pesticides have, roughly speaking, the same size, as a consequence the corresponding computed values of  $D_s$  are close.

The surface diffusivity for diuron is however significantly smaller than for atrazine and bromoxynil. On the other hand, the isotherm data showed that the GAC adsorption capacity for diuron is about 20% greater than for the two other pesticides. Thus, in a drinking water plant, even if the amount of diuron that could potentially be trapped by the activated carbon is more important than the amounts of atrazine and bromoxynil, it may not have enough contact time to be adsorbed. This clearly points out the need of rate studies for plant design and operation, in addition to equilibrium experiments. Of course, competition between several compounds (natural matter or contaminants) will also modify the adsorption (Gicquel et al., 1997) but this goes beyond the scope of this paper.

## Conclusions

The differential column batch reactor associated with the Homogeneous Surface Diffusion Model appears to

be an efficient system for the determination of surface diffusion coefficients for granular activated carbon. Compared to stirred reactors, the range of obtainable  $D_s$  values has been increased by an order of magnitude. A better knowledge and control of the external transfer coefficient  $k_f$ , a narrower  $k_f$  distribution throughout the reactor, result in a greater precision of the estimated surface diffusivities. A rough confidence interval could also be proposed, based on the experimental error and the model sensitivity with respect to the diffusion coefficient.

## Nomenclature

$C$	Liquid concentration ( $\mu\text{g} \cdot \text{L}^{-1}$ )
$C_0$	Initial liquid concentration ( $\mu\text{g} \cdot \text{L}^{-1}$ )
$C_b$	Liquid concentration in the bulk ( $\mu\text{g} \cdot \text{L}^{-1}$ )
$C_s$	Liquid concentration at liquid/solid interface ( $\mu\text{g} \cdot \text{L}^{-1}$ )
$D_{\text{mol}}$	Molecular diffusion coefficient ( $\text{cm}^2 \cdot \text{s}^{-1}$ )
$D_p$	Pore diffusion coefficient ( $\text{cm}^2 \cdot \text{s}^{-1}$ )
$D_s$	Surface diffusion coefficient ( $\text{cm}^2 \cdot \text{s}^{-1}$ )
$K$	Freundlich coefficient
$k_f$	External mass transfer coefficient ( $\text{cm} \cdot \text{s}^{-1}$ )
$n$	Freundlich coefficient
$q$	Absorbate load ( $\mu\text{g} \cdot \text{mg}^{-1}$ )
$q_0$	Initial absorbate load ( $\mu\text{g} \cdot \text{mg}^{-1}$ )
$Q_0^*$	Absorbate load in equilibrium with $C_0$ ( $\mu\text{g} \cdot \text{mg}^{-1}$ )
$q_{\text{avg}}$	Average absorbate load ( $\mu\text{g} \cdot \text{mg}^{-1}$ )
$q_s$	Absorbate load at liquid/solid interface ( $\mu\text{g} \cdot \text{mg}^{-1}$ )
$r$	Radial distance inside the particle of adsorbent (m)
$R_p$	Radius of adsorbent particle (m)
$t$	Time (s)
$U_0$	Superficial velocity ( $\text{m} \cdot \text{s}^{-1}$ )
$W$	GAC dosage ( $\text{mg} \cdot \text{L}^{-1}$ )
$\rho$	Liquid density ( $\text{g} \cdot \text{L}^{-1}$ )
$\rho_a$	Apparent adsorbent density ( $\text{g} \cdot \text{L}^{-1}$ )
$\mu$	Liquid viscosity, Pa·s
Biot	Biot Number = $\frac{k_f R_p C_0}{D_s \rho_a Q_0^*}$
Sh	Sherwood Number = $\frac{2 R_p k_f}{D_{\text{mol}}}$
Sc	Schmidt Number = $\frac{\mu}{\rho D_{\text{mol}}}$
Re	Reynolds Number = $\frac{2 R_p \rho U_0}{\mu}$

## References

- Al Duri, B., "Adsorption Modelling and Mass Transfer," *Use of Adsorbents for the Removal of Pollutants from Wastewaters*, Ch. 7, pp. 133–173, CRC Press, 1996.
- Crittenden, J.C., D.W. Hand, H. Arora, and B.W. Lykins, "Considerations for GAC Treatment of Organic Chemicals," *J. Am. Water Works Assoc.*, **79**(1), 74–82 (1987).
- Ganguly, S.K. and A.N. Goswamy, "Surface Diffusion Kinetics in the Adsorption of Acetic Acid on Activated Carbon," *Sep. Sci. Technol.*, **31**(9), 1267–1278 (1996).
- Gicquel, L., D. Wolbert, and A. Laplanche, "Adsorption of Atrazine by Powdered Activated Carbon: Influence of Dissolved Organic and Mineral Matter of Natural Waters," *Environ. Technol.*, **18**, 467–478 (1997).
- Hand, D.W., J.C. Crittenden, and W.E. Thacker, "User-Oriented Batch Reactor Solutions to the Homogeneous Surface Diffusion Model," *J. Environ. Eng. Div.*, **109**(1), 82–101 (1983).
- Komiyama, H. and J.M. Smith, "Surface Diffusion in Liquid-Filled Pores," *AIChE J.*, **20**(6), 1110–1117 (1974).
- McKay, G. and B. Al Duri, "Multicomponent Dye Adsorption onto Carbon Using a Solid Diffusion Mass-Transfer Model," *Ind. Eng. Chem. Res.*, **30**(2), 385–395 (1991).
- Noll, K.E., V. Gouranis, and W.S. Hou, *Adsorption Technology for Air and Water Pollution Control*, Lewis Publishers, 1992.
- Qi, S., S.S. Adham, V.L. Snoeyink, and B.W. Lykins, "Prediction and Verification of Atrazine Adsorption by PAC," *J. Environ. Eng. Div.*, **120**(1), 202–218 (1994).
- Rosen, J.B., "Kinetics in a Fixed Bed System for a Solid Diffusion into Spherical Particles," *J. Chem. Phys.*, **20**(3), 387–394 (1952).
- Roy, D., G.T. Wang, and D.D. Adrian, "A Simplified Solution Technique for Carbon Adsorption Model," *Water Res.*, **27**(6), 1033–1040 (1993).
- Ruthven, D.M., *Principles of Adsorption and Adsorption Processes*, Wiley & Sons Publishers, USA, 1984.
- Tien, C., *Adsorption Calculations and Modeling*, Butterworth-Heinemann Series in Chemical Engineering, Butterworth-Heinemann Publishers, USA, 1994.
- Traegner, U.K. and M.T. Suidan, "Parameter Evaluation for Carbon Adsorption," *J. Environ. Eng. Div.*, **115**(12), 109–128 (1989).
- Villadsen, J.V. and W.E. Stewart, "Solution of Boundary-Value Problems by Orthogonal Collocations," *Chem. Eng. Sci.*, **22**, 1483–1501 (1978).
- Wakao, N. and T. Funazkri, "Effect of Fluid Dispersion Coefficients on Particle-to-Fluid Mass Transfer Coefficients in Packed Beds," *Chem. Eng. Sci.*, **33**, 1375–1384 (1978).
- Walker, G.M. and L.R. Weatherley, "Kinetics of Acid Dyes Adsorption onto GAC," *Water Res.*, **33**(8), 1895–1899 (1999).
- Weber, T.W. and R.K. Chakravorti, "Pore and Solid Diffusion Models for Fixed-Bed Adsorbents," *AIChE J.*, **20**(2), 228–238 (1974).
- Weber, W.J. and J.M. Smith, "Simulation and Design Models for Adsorption Processes," *Environ. Sci. Technol.*, **21**(11), 1040–1050 (1987).
- Zhou, M.L., *Modélisation de l'absorption sur charbon actif*, PhD Thesis, University of Rennes 1, France, 1992.
- Zhou, M.L. and G. Martin, "Adsorption Kinetics Modelling in Batch Reactor onto Activated Carbon by the Model HSDM," *Environ. Technol.*, **16**, 827–838 (1995).